

Atomically dispersed vanadium oxides on multiwalled carbon nanotubes via atomic layer deposition: A multiparameter optimization

Pascal Dungen, Mark Greiner, Karl-Heinz Böhm, Ioannis Spanos, Xing Huang, Alexander A. Auer, Robert Schlögl, and Saskia Heumann

Citation: *Journal of Vacuum Science & Technology A: Vacuum, Surfaces, and Films* **36**, 01A126 (2018);

View online: <https://doi.org/10.1116/1.5006783>

View Table of Contents: <http://avs.scitation.org/toc/jva/36/1>

Published by the [American Vacuum Society](#)

Articles you may be interested in

[Plasma enhanced atomic layer deposition of aluminum sulfide thin films](#)

Journal of Vacuum Science & Technology A: Vacuum, Surfaces, and Films **36**, 01A113 (2017);
10.1116/1.5003339

[Influence of N₂/H₂ and N₂ plasma on binary III-nitride films prepared by hollow-cathode plasma-assisted atomic layer deposition](#)

Journal of Vacuum Science & Technology A: Vacuum, Surfaces, and Films **36**, 01A110 (2017);
10.1116/1.4998920

[Spatial atomic layer deposition for coating flexible porous Li-ion battery electrodes](#)

Journal of Vacuum Science & Technology A: Vacuum, Surfaces, and Films **36**, 01A123 (2017);
10.1116/1.5006670

[Atomic layer deposition of molybdenum disulfide films using MoF₆ and H₂S](#)


Journal of Vacuum Science & Technology A: Vacuum, Surfaces, and Films **36**, 01A125 (2017);
10.1116/1.5003423

[Review Article: Catalysts design and synthesis via selective atomic layer deposition](#)

Journal of Vacuum Science & Technology A: Vacuum, Surfaces, and Films **36**, 010801 (2017);
10.1116/1.5000587

[Nucleation mechanism during WS₂ plasma enhanced atomic layer deposition on amorphous Al₂O₃ and sapphire substrates](#)

Journal of Vacuum Science & Technology A: Vacuum, Surfaces, and Films **36**, 01A105 (2017);
10.1116/1.5003361



Instruments for Advanced Science


Contact Hiden Analytical for further details:
W www.HidenAnalytical.com
E info@hiden.co.uk

CLICK TO VIEW our product catalogue




Gas Analysis

- dynamic measurement of reaction gas streams
- catalysis and thermal analysis
- molecular beam studies
- dissolved species probes
- fermentation, environmental and ecological studies




Surface Science

- UHV TPD
- SIMS
- end point detection in ion beam etch
- elemental imaging - surface mapping



Plasma Diagnostics

- plasma source characterization
- etch and deposition process reaction kinetic studies
- analysis of neutral and radical species



Vacuum Analysis

- partial pressure measurement and control of process gases
- reactive sputter process control
- vacuum diagnostics
- vacuum coating process monitoring

Atomically dispersed vanadium oxides on multiwalled carbon nanotubes via atomic layer deposition: A multiparameter optimization

Pascal Dünge, Mark Greiner, Karl-Heinz Böhm, and Ioannis Spanos
Max-Planck-Institut für Chemische Energiekonversion, Stiftstraße 34-36, 45470 Mülheim an der Ruhr, Germany

Xing Huang
Fritz-Haber-Institut der Max-Planck-Gesellschaft, Faradayweg 4-6, 14195 Berlin, Germany

Alexander A. Auer
Max-Planck-Institut für Chemische Energiekonversion, Stiftstraße 34-36, 45470 Mülheim an der Ruhr, Germany

Robert Schlögl
Max-Planck-Institut für Chemische Energiekonversion, Stiftstraße 34-36, 45470 Mülheim an der Ruhr, Germany and Fritz-Haber-Institut der Max-Planck-Gesellschaft, Faradayweg 4-6, 14195 Berlin, Germany

Saskia Heumann^{a)}
Max-Planck-Institut für Chemische Energiekonversion, Stiftstraße 34-36, 45470 Mülheim an der Ruhr, Germany

(Received 27 September 2017; accepted 4 December 2017; published 29 December 2017)

The focus of the present work is to investigate the bonding characteristics of vanadium oxide species to different oxygen functional groups on multiwalled carbon nanotubes (MWCNT). Atomic layer deposition (ALD) was used to deposit atomically dispersed vanadium oxide species on MWCNT. To generate atomically dispersed vanadium, only one ALD cycle was applied for the deposition of vanadium. The MWCNT functional groups that are involved in the deposition process were identified by thermal analysis and grafting experiments. A variety of ALD process parameters were tested, and revealed that purging times between dosing of vanadium precursor and dosing of water as coreactant had a strong influence on the ratio of vanadium species that are physisorbed or chemisorbed to the MWCNT. The ALD process parameters were optimized to focus on the immobilization of the vanadium due to a chemical bond between vanadium species and MWCNT. Because of the direct correlation between catalytic stability and immobility of the vanadium species, the importance of knowledge about the influence of the ALD parameter onto the bond formation is essential. Raman spectroscopy and high resolution scanning transmission electron microscopy images were used to prove the single site structure of the vanadium oxide. © 2017 Author(s). All article content, except where otherwise noted, is licensed under a Creative Commons Attribution (CC BY) license (<http://creativecommons.org/licenses/by/4.0/>). <https://doi.org/10.1116/1.5006783>

I. INTRODUCTION

Carbon nanotubes (CNT) are potentially useful support materials for (electro)catalysts due to the inert and electrically conductive nature. In order to exhibit catalytic activity, CNT must be functionalized and chemically active moieties, such as a metal or metal oxide has to be added. However, in order to withstand many thousands of hours of catalytic operation, such moieties must be strongly bounded to the CNT surface. This requirement has proven thus far more difficult to fulfill than anticipated and has revealed a gap in knowledge of how metal-oxide functional groups bind to CNT.

Atomic layer deposition (ALD) is a suitable technique for depositing metal oxide films on graphitic materials like carbon nanotubes.¹⁻⁵ The alternating pulses of metal precursor and oxygen source, as well as the self-limiting character of the reaction, enable uniform coating of surfaces with extremely high aspect ratios. Increasing the number of deposition cycles, the conformity of the metal film increases.

A prerequisite for depositing metal oxides is the presence of functional groups on the carbon surface. Functional groups act as anchor sites for metal oxide precursors and must be generated prior to precursor dosing via a surface treatment of the carbon material. In the literature, several studies discuss the formation of conformal metal oxide films on carbon materials for a variety of applications.⁵⁻⁹ The stability of such films in a given application is important for stable performance. Oxide agglomerations and defects, resulting from weak interactions between the deposited species and the base material, decrease film stability during operation. Such sources of instability need to be rectified for oxide-functionalized multiwalled carbon nanotube (MWCNT) to be used in any application.

The process parameters used in ALD have a strong influence on the structure and composition of the resulting material. Such parameters must always be tested when new procedures are developed, in order to verify that the deposition process is truly ALD. We have verified herein that the deposition of the vanadium precursor [vanadium(V)-oxyisopropoxide] on functionalized multiwalled carbon nanotube (MWCNT) is an ALD process. Subject to this finding, we tested the influence of

^{a)}Electronic mail: saskia.heumann@cec.mpg.de

TABLE I. Characteristics of untreated MWCNTs.

Specific surface area (N ₂ sorption)	232 m ² /g
Length	3–12 μm
Outer diameter	12.9 ± 3.5 nm
Wall thickness	4.1 ± 1.3 nm
Wall No.	8–15
D*/G ratio (Raman)	1.4
Carbon content	97.1%
Mass loss during thermal treatment up to 900 °C	2.5 wt. %

various ALD parameters on the consumption of various MWCNT functional groups to verify their ALD activity. The influence of temperature, precursor exposure time, pressure and time between vanadium precursor and oxygen source pulses during the deposition were considered. In the present study, we have employed a new strategy to study ALD activity of functional groups via thermogravimetric analysis, density functional theory calculations, and grafting experiments. Namely, we have synthesized atomically dispersed catalysts in order to avoid the influence of neighboring vanadium oxide groups that occurs on heavily functionalized nanotubes. Atomically dispersed vanadium oxide was reached by applying only one ALD cycle during the deposition. By eliminating the influence of neighboring groups, we can examine the interaction between metal species and the base material without the complications of secondary processes, allowing for a clearer answer to fundamental catalytic questions regarding the ALD activity of functional groups.

II. EXPERIMENT

A. Functionalization of MWCNT

MWCNT produced from Shangdong Dazhang Nano Materials, Co., were treated with nitrosulfuric acid (NSA) (vol. % ratio: 1:1; nitric acid 65%:sulfuric acid 98%) to generate oxygen containing functional groups on the MWCNT surface. Therefore, 10 g of carbon materials were mixed with 500 ml acid at 105 °C for 4 h under continuous stirring. Resulting nitrous gases were neutralized with 3 mol/l NaOH solution. Afterward, the partially oxidized carbon materials were filtered and the excess of acid and catalyst residues without reacting were washed out over several hours in a washing cell. Additionally, 10 g MWCNT without functional groups was prepared as reference by a hydrochloric acid treatment

at 105 °C for 24 h under continuous stirring and likewise subsequent washing procedure. Functionalized MWCNTs were dried in a vacuum oven at 80 °C for 12 h to eliminate residual water.¹⁰ Before its use as a support material in the ALD process, MWCNTs were annealed (under inert atmosphere) at defined temperatures to remove specific functional groups. Table I lists some properties of untreated MWCNT to give a detailed view of the support material character.

Present defects in the MWCNT structure determined via Raman spectroscopy mainly results out of carbon rings different from six ring structures like, for example, Stone-Wales-Defects,¹¹ or carbon atoms which exhibits less than three neighboring carbon atoms. These carbon atoms are mostly saturated with hydrogen or oxygen. This saturation was also determined via analyzing the carbon content. The residual amount of noncarbon content of 2.9% is mainly attributed to hydrogen as well as traces of oxygen and metal catalysts.

B. Atomic layer deposition

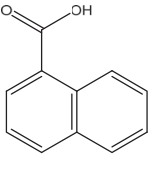
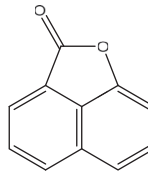
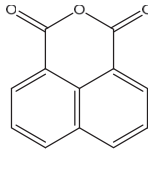
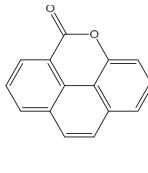
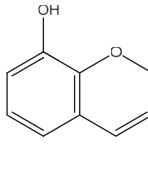
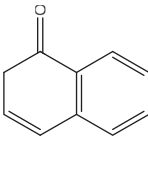
A commercial ALD (Savannah S200, Ultratech) was used to deposit vanadium oxide on carbon materials. Vanadium-oxytriisopropoxide (CAS: 5588-84-1, Sigma-Aldrich) precursor was heated to 70 °C and exposed for 0.05 up to 0.65 s. The deposition temperature varied between 130 and 170 °C inside of the known ALD window.¹² To extend the exposure time without influencing the pressure inside the chamber, constant precursor pulses were dosed into the chamber. After 40 s exposure, the chamber was pumped down to base pressure and the precursor was pulsed again. Due to the repeated precursor pulses, the total exposure time can be increased. Water used as an oxygen source was pulsed for 0.09 s with the same repetitions like the metal precursor pulses. The detailed deposition procedure is shown in the supplementary material.¹³

C. Thermogravimetric mass spectroscopy

A STA 449 F3 Jupiter[®] QMS4 from Netzsch with an argon gas flow of 70 ml/min was used for the thermogravimetric mass spectroscopy (TG-MS) analysis. A stepwise heating rate was used to investigate the interaction of the vanadium precursor and different functional groups. Table II shows the assignment of decomposing products connected to decomposition temperatures and species of functional groups.

The functionalized MWCNT samples were heated at specific deposition temperature for the ALD process in the ALD

TABLE II. Decomposition temperature of different functional groups on MWCNT (Refs. 14–18).

	Carboxylic	Lactone (zig-zag)	Anhydride	Lactone (arm-chair)	Phenol ether	Carbonyl
Decomposition temp. (°C)	>253	253–315	315–620	510–620	620–800	800–1000
Isothermal step	1	2	3–4	4–5	5	6
Structure						
Signal	CO ₂	CO ₂	CO ₂ + CO	CO	CO	CO

chamber. Afterward, a part of the sample was removed to analyze the remaining functional groups via TG-MS. The rest of the sample was exposed during the ALD treatment with vanadium precursor and coreactant. This sample was also analyzed by TG-MS. The weight-normalized ion currents of both measurements were subtracted from each other to determine the consumption of each functional group.

D. Raman spectroscopy

To record Raman spectra, a Thermo Scientific DXR Raman Microscope (Germany) with a 50× magnification and 532 nm laser was used. The samples were measured within 10 s and eight exposures. The laser power was 1.1 mW. If vanadium oxide is present on the MWCNT as single sites, one would expect not measureable Raman signal because such species exhibit no lattice vibrations. Thus, to prove the presence of vanadium oxide on the MWCNT surface, one must modify the analysis procedure. In order to obtain a Raman signal, we stimulated the formation of a vanadium oxide lattice via intentional radiation damage. The laser power was increased after every measurement up to 10 mW, and the exposure time was extended to 10 s with 16 exposures. Under these measurement conditions, beam damage causes particle agglomerations and forms V_2O_5 . The appearing lattice vibration proves that vanadium is present on the measured spot. To ensure that the low power Raman method is able to detect lattice vibrations, the same spot was measured again, after the induced radiation damage, using the former low-power method. Appearing lattice vibrations show the practicability of the low laser power Raman method to detect V_2O_5 and to prove the existence of vanadium oxide single site on the MWCNT surface.

E. ICP-OES

A vanadium-containing solution was continuously streamed into the inductive coupled plasma optical emission spectroscopy (ICP-OES) (Spectroblue EOP, Ametek) by means of a peristaltic pump at a flow rate of 0.18 ml/min through a quartz nebulizer operating at nebulizer gas flow rates of 0.85 l/min (Ar, purity 99.999%). Three single measurements were recorded with an integration interval of 100 ms and two sweeps per reading. The detection limits are in the order of 0.1 ppb of metal according to the manufacturer. Calibration was performed using seven standard solutions [100, 50, 10, 5, 1, 0.5, and 0 (as a blank solution) ppm metal, prepared from Merck Certi-PUR®]. Finally the RF power was set to 1400 W with a plasma gas flow rate of 15 l/min.

F. Atomic absorption spectroscopy

This method was an external service measurement by Mikrolab Kolbe; this laboratory is specialized on the determination of metal contents of carbonous samples. The vanadium oxide containing MWCNT were digested in a mixture of hydrochloric and hydrogen peroxide. The solution was analyzed via atomic absorption spectroscopy (AAS).

G. Grafting

Grafting experiments show the reactivity of vanadium(V) oxytriisopropoxide with different organic molecules in organic solvents. During the experiment vanadium(V) triisopropoxide was mixed with different educts in chloroform. All experiments were done in a glovebox. For further experiments, the chloroform was evaporated under vacuum, leftovers were solved in different solvents, filtered, and measured via ^{51}V -NMR.

H. DFT calculations

Density functional theory (DFT) calculations were carried out using a two-layer carbon model incorporating either anhydride, hydroxyl, carbon acid or lactone groups (optimized at the RI BP86- D3/def2-TZVP level of theory) to determine the reaction energies of the vanadium precursor. Detailed information can be found in the supplementary material.

III. RESULTS AND DISCUSSION

Before investigating how parameter changes influence the deposition process, it is important to verify that the deposition process is truly an ALD process (i.e., a self-limiting process). To verify this, we progressively increased the vanadium precursor exposure time until all ALD-active functional groups were saturated, as determined via postanalysis by measuring the vanadium concentration with AAS. After consuming all functional groups, further increase in exposure time did not result in additional vanadium oxide deposition. By depositing onto two different pretreated MWCNTs, we tested for the necessity of functional groups as anchor sites for the vanadium precursor. Hydrochloric acid (HCl) functionalized MWCNT do not provide functional groups, whereas NSA treatment produces a variety of functional groups on the MWCNT surface—such as carboxy, lactone, anhydride, phenol, ether, and carbonyl groups.^{14–18} The density of functional groups of NSA treated MWCNTs is nevertheless sparsely populated on the surface. The D^*/G ratio by Raman spectroscopy was determined by focusing on single phonon resonances which is only possible in highly graphitic materials.¹⁰ The high inert carbon content (low D^*/G ratio) and structural properties emphasize that long diffusion times are necessary to guarantee contact between precursor and all available active sites, which are located at defect sites in the graphitic lattice. The high surface area and tubular structure of the MWCNT impede the deposition of vanadium oxide via ALD. Additionally, high purging times are necessary to avoid gas phase reactions of the precursor [vanadium(V) isopropoxide and water], which often occur in chemical vapor deposition (CVD) approaches. A CVD reaction results in nonselective deposition over the whole surface without covalent bond formation between support and precursor species.

Figure 1 demonstrates the self-limiting character of the ALD process. Both base materials—i.e., the nitrosulfuric (inverted triangles in Fig. 1) and hydrochloric acid (triangles in Fig. 1) pretreated MWCNT—exhibit saturation after 1500 exposures. The observation of saturation demonstrates the chemical inertness of the vanadium precursor toward itself. Unexpectedly, the HCl-treated MWCNT consumes a greater

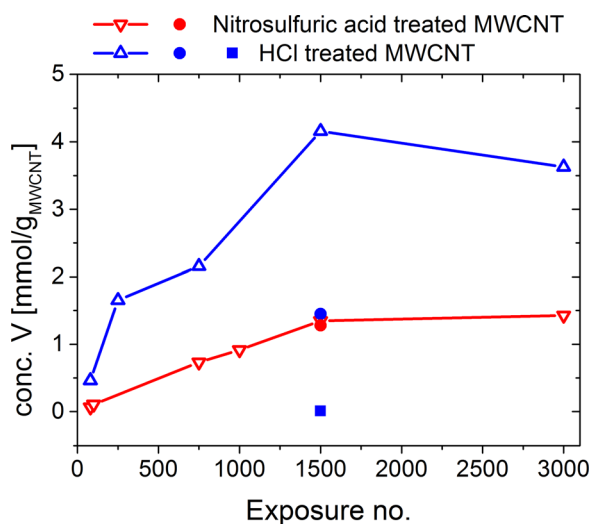


Fig. 1. (Color online) Effect of different MWCNT pretreatments on the vanadium oxide deposition. Hydrochloric acid pretreated (triangles) with less functional groups and nitrosulfuric acid pretreated MWCNT (inverted triangles) were exposed to the vanadium precursor. The deposited amount of vanadium was detected via AAS. The exposing number increases till the deposited amount of vanadium oxide becomes constant. The influence of purging time of 24 h (circles) and 48 h (rectangles) between vanadium precursor and coreactant pulse was also investigated.

amount of vanadium precursor than NSA-treated MWCNT. Vanadium oxide loadings were 4.2 and 1.4 mmol/g for HCl- and NSA-treated MWCNT, respectively. This is a peculiar finding, given that HCl-treated MWCNTs do not have a significant amount of functional groups for the precursor to react with. This contradiction suggests that the apparent saturation level does not guarantee that a process is ALD, as we demonstrate through subsequent experimentation. Chloride residual in the MWCNT samples were not found after the HCl-treatment (XPS), and in turn the higher quantity of deposited vanadium species cannot be traced back to a reaction between the vanadium precursor and HCl.

By increasing the purging times between the vanadium precursor pulses and the water pulses, the amount of vanadium precursor deposited onto the HCl-treated MWCNT decreases (see Fig. 1, blue circle: 24 h purge; blue rectangle: 48 h purge). In contrast, increasing the purging time had no effect on the amount of vanadium deposited onto NSA-treated MWCNT (see Fig. 1, red rectangle: 48 h purge). This finding suggests that the vanadium oxide on the HCl-treated MWCNT was actually only physisorbed after 2 h of purging, rather than chemically attached to the MWCNT surface. The influence of shorter purging times on the amount of physisorbed vanadium precursor on NSA-treated MWCNT is discussed later (Fig. 7).

Due to the high surface area of the MWCNT, the vanadium oxide precursor does not completely desorb after 24 h of purging. The water pulses are found to immobilize the excess of physisorbed precursor, such that after water pulsing, the precursors are not easily removed by purging. If sufficiently purged before the water pulses, in this case 48 h, nearly all of the physisorbed vanadium precursor can be removed from the hydrochloric acid pretreated MWCNT. This finding shows that, in fact, no ALD of the vanadium

precursor had occurred on the HCl-treated MWCNT. In the case of NSA-treated MWCNT, purging times had no influence on the amount of deposited vanadium because all the vanadium precursor present in the pulse was chemically bounded to the MWCNT surface and could not be desorbed.

The deposition on different base materials demonstrates the importance of adequate purging times between metal precursor and oxygen source pulses. If insufficient purging times are used, one can erroneously come to the conclusion that an ALD process is taking place. Furthermore, it is obvious that the optimal time between the different precursor pulses is not only related to the characteristics of the metal precursor but also to the characteristics of the support material.

For the subsequent experiments shown in this work, only the nitrosulfuric acid pretreated MWCNT were used because this pretreatment ensures an ALD process in sense of the formation of a chemical bond between the vanadium precursor and MWCNT. The investigation of the ALD-active functional groups was made via TG-MS measurements (supplementary material). The experimental procedure is illustrated in supplementary material, Figs. S1–S5. A summary of the functional group consumption during the ALD is shown in Fig. 2.

Figure 2 illustrates the activity of different functional groups during the ALD process. Carboxyl, anhydride, and phenol groups show significant consumption due to their reactivity with the vanadium precursor, whereas lactone groups appear to be inactive. Since the vanadium oxide species deposited on the MWCNT are reduced at temperatures over 800 °C, the analysis of the reactivity of carbonyl groups is not possible via TG-MS. A detailed discussion regarding the consumption of different functional groups and their interactions with deposited vanadium oxide on MWCNT during thermal analysis is provided in the supplementary material.

Additionally, grafting experiments between vanadium(V) oxyisopropoxide and model substances with similar functional groups present on MWCNT were performed to confirm the results found in our TG-MS studies. To this end,

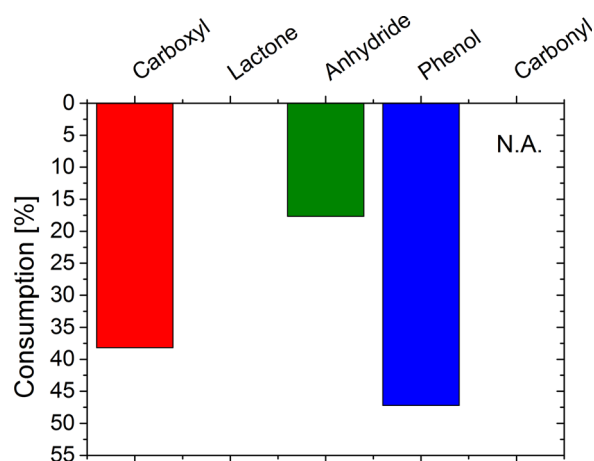


Fig. 2. (Color online) Consumption of different functional groups during the ALD procedure analyzed via TG-MS. Carboxylic, anhydride, and phenol groups exhibit a reduction in the peak areas after the ALD process in the TG-MS measurements, whereas lactone groups are not affected. A consumption of carbonyl groups could not be analyzed due to interactions between vanadium oxide and MWCNT at this temperature range.

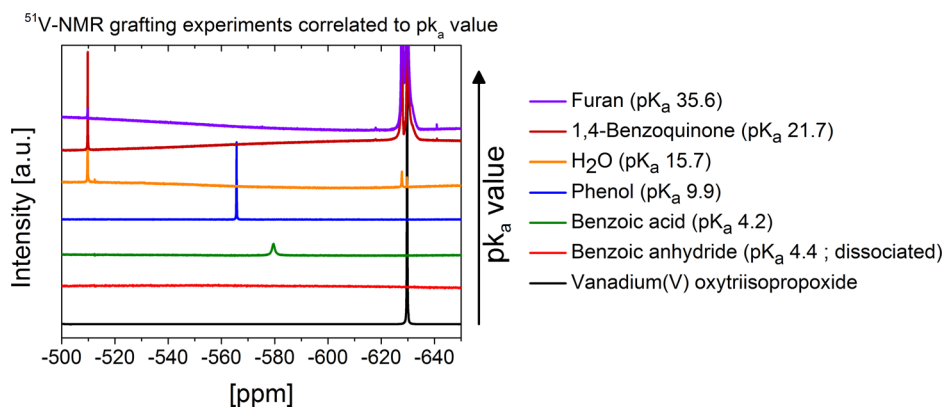


FIG. 3. (Color online) ^{51}V -NMR after grafting experiments with different reaction educts as model substances with vanadium(V) oxyisopropoxide.

molecules with different pK_a values were mixed with the precursor in liquid phase under inert atmosphere, and the vanadium species produced were isolated and analyzed via ^{51}V -NMR. Figure 3 shows the grafting results correlated with the pK_a values of the reactants.

Vanadium(V) triisopropoxide exhibits a NMR shift of -629.8 ppm (black) and is representative of a grafting experiment without reaction. Benzoic acid (-579.5 ppm, green), phenol (-565.7 ppm, blue), and water (-509.8 , orange) exhibit NMR shifts which indicate a reaction with the precursor. Further increasing the pK_a to 1,4-benzoquinone and furan, no reaction between educts and precursor takes place. The appearing shifts result from water contamination of the educts. Benzoic anhydride also shows no reaction with vanadium precursor during grafting experiments even though the pK_a suggests a reaction should occur. However, the absence of water during the grafting experiment hinders the dissociation of anhydride, prohibiting the reaction. To gain deeper knowledge into the apparent reaction and to confirm the ligand exchange of the vanadium precursor to form a covalent bond with phenol, ^1H -NMR spectra of the reaction with phenol (highest pK_a value) were collected and analyzed. Here, we were able to distinguish between bound isopropyl and free isopropanol,

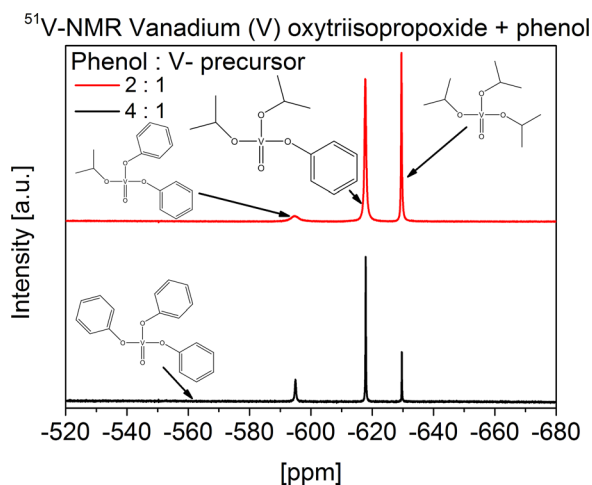


FIG. 4. (Color online) ^{51}V -NMR of grafting experiments with different molar ratios between the vanadium(V) oxytriisopropoxide precursor and phenol as representative for phenol groups.

as well as between bound phenyl and free phenol. The experiments were fulfilled with different molar ratios between vanadium(V) oxyisopropoxide and phenol, showing that partial as well as complete exchange of organic ligands takes place in dependence of the molar ratio (Fig. 4). Furthermore, the reversibility of the reaction was demonstrated (supplementary material, S8).

We have performed a series of calculations which support our results for the activity of different functional groups as elucidated from TG-MS and grafting experiments. In order to assess the thermodynamics of the reactions involved in the ALD process, electronic structure calculations were carried out using density functional theory for a series of molecular models for the reaction of vanadium(V) triisopropoxide.

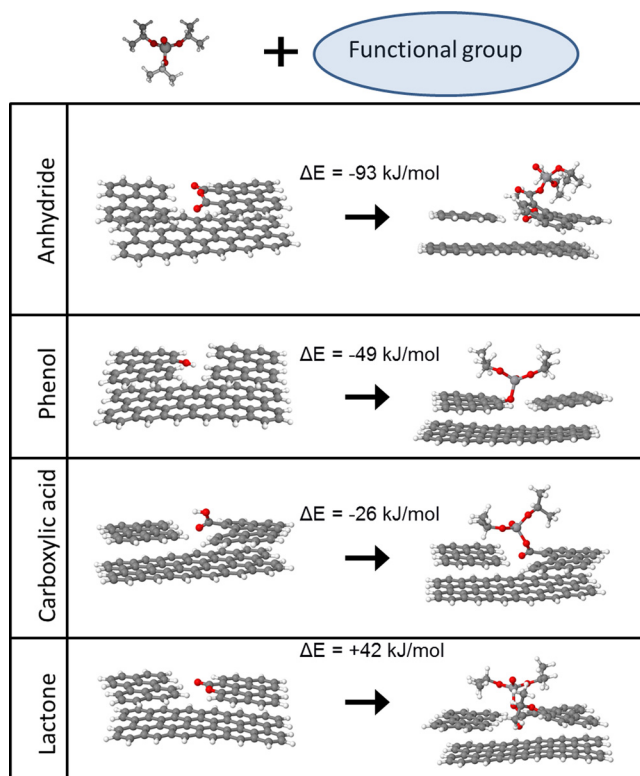


FIG. 5. (Color online) Calculated reaction energies of different functional groups located on a two-layer carbon model with vanadium(V) oxytriisopropoxide.

For this purpose, reaction energies of the vanadium precursor were determined with the use of a two-layer carbon model incorporating either anhydride, hydroxyl, carbon acid, or lactone groups. These structures and a summary of our results are provided in Fig. 5.

The calculated results are in agreement with what we have observed experimentally, showing that the most stable product is formed with anhydride, while the reaction with the lactone is even endothermic and hence highly unfavorable. While the reaction of the carboxylic acid is still slightly exothermic, a value around -20 kJ/mol is within the error bars of the computational model and the reaction is probably unfavorable or sluggish. Concluding thus far, the reaction of vanadium(V) triisopropoxide with carboxylic, anhydride, and phenol groups and the related substitution of vanadium precursor ligands has been investigated through a combination of TG-MS, grafting, and DFT calculations. Additionally, the self-limitation during the ALD process was strongly supported by our AAS experiments (Fig. 1).

We continue this study with a deeper investigation into the influence of ALD parameters by analyzing the consumption of carboxylic groups. Note: anhydride and phenol groups were not chosen for further analysis because of the weaker influence of temperature on the consumption of anhydride groups and the poorer signal-noise ratio during the detection of the phenol group consumption (supplementary material). Figure 6 demonstrates the influence of pressure, exposure time to vanadium precursor, and deposition temperature as variable ALD parameters.

Figure 6(a) shows the integrated CO_2 decreasing upon ALD determined by TG-MS analysis, which is taken to represent the carboxylic group consumption by the ALD process. The deposition temperature of 150°C (red bar) exhibits the highest consumption. At this temperature, with increasing vanadium precursor pulse times, up to 0.35 s, the consumption continues increasing. Further increases of pulse time decrease the consumption. In the case of the deposition at 130°C (green bar), increasing pulse times actually decreases the consumption. The pulse time has a negligible influence on the carboxylic group consumption during a deposition at 170°C .

The decreased consumption with increasing pulse times during the deposition at 130 and 150°C could be explained by the increase in pressure that accompanies increasing the pulse time. The results lead to the assumption that, due to higher pressure, the accessibility of pores for the precursor decreases.¹⁹ Additionally, with higher fluxes, the contact between vanadium precursor and MWCNT gets reduced due to the reactor design of the ALD setup, whereby the vanadium precursor is transported by a gas flux which is parallel to the sample. The deposition temperature of 150°C illustrates the two opposing influences of the parameters pulse time and pressure. Increasing pulse times, the vanadium precursor concentration inside the ALD chamber increases. Thereby more vanadium reacts with the carboxylic groups. On the other hand, the pressure—which consists primarily of carrier gas—inhibits the consumption of the carboxylic group.

To emphasize this trend, an additional data point with a pulse time of 0.05 s was measured at the deposition temperature of 150°C . The influence of the pressure inhibition is more pronounced at lower deposition temperatures. The decreased carboxylic group consumption, as well as the reduced influence of pressure during the deposition at 170°C , can be explained by a partial decomposition of the vanadium precursor at this temperature. (Refer to MS spectra in the supplementary material.) The described trends of the carboxylic group consumption cannot be observed by the detection of the deposited amount of vanadium via AAS [Fig. 6(b)], in which the deposited amount of vanadium increases with the pulse time. AAS analysis suggests that the ideal deposition temperature for vanadium oxide via ALD is 130°C , which results in the highest vanadium oxide concentration on the MWCNT surface. In contrast to TG-MS analysis, AAS can give no information about the bonding properties of the deposited vanadium oxide. Combining both techniques (TG-MS and AAS) shows that the desorption rate of physisorbed vanadium oxide is lower at 130°C compared to 150°C , which results in a higher deposition but less carboxylic group consumption. To generate vanadium oxide, which is bonded on the MWCNT surface, temperature at 150°C exhibits the best results unless the total amount of deposition is lower compared to lower deposition temperatures.

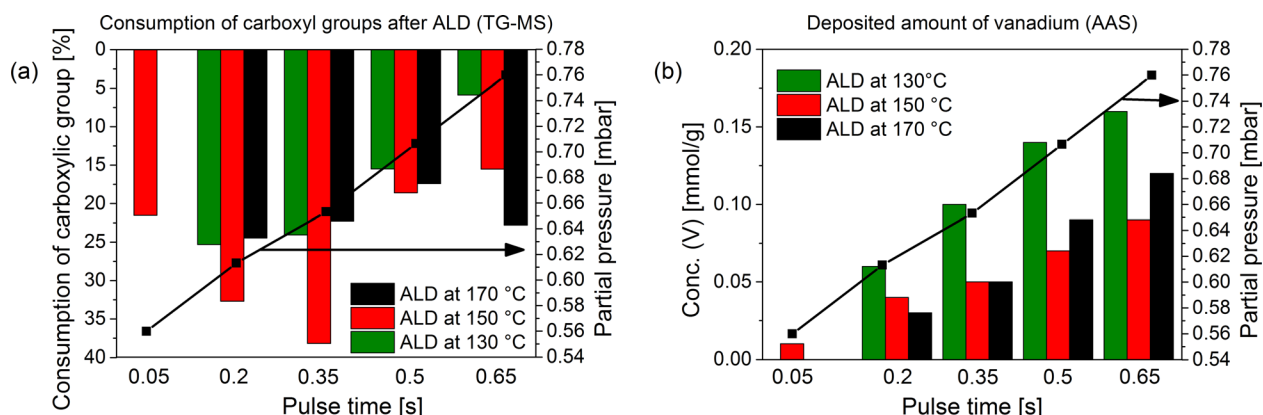


Fig. 6. (Color online) (a) Consumption of carboxylic group correlated to parameter changes (temperature, pressure and exposure time) during the ALD procedure analyzed via TG-MS. (b) Deposited amount of vanadium oxide determined via AAS.

As described earlier, with the comparison of NSA- and HCl-treated MWCNT, with insufficient purging times, vanadium precursors can become physisorbed to the MWCNT surface. Figure 6 illustrates the influence of the total deposited amount of vanadium oxide when the purging time between the precursor pulses is decreased. With this approach, we can determine the amount of chemically bonded and physisorbed part of the vanadium oxide.

The total amount of physisorbed (CVD) and chemisorbed (ALD) vanadium oxides was determined by mixing the vanadium oxide containing MWCNT with water or acid, followed by filtration of the MWCNT and ICP-OES measurements of the resulting supernatant. The Pourbaix diagram (supplementary material) of vanadium illustrates the vanadium species appearing at different pH values in dependence to an applied potential. It exhibits that vanadium oxide species are soluble under acidic conditions (without applying a potential), whereby covalent bonds between vanadium oxide and MWCNT surface are also hydrolyzed. Hydrolyzation of covalently bonded vanadium species will not take part at higher pH values. Nevertheless, physisorbed vanadium oxides can be dissolved at low and higher pH values due to weaker interactions between MWCNT and vanadium species. The ratio between physisorbed and chemisorbed vanadium oxide species could be therefore determined by the measured amount of soluble vanadium in acid and water, as shown in Fig. 7.

Also, the influence of the repetition of vanadium precursor pulses to extend the exposure time without increasing the pressure was investigated. The time between the vanadium precursor pulses was held constant at 112 s, while the purging time before the water pulse was varied between 1 and 7200 s. The purging time has no significant influence on the amount of water soluble (physisorbed) vanadium species when the MWCNT surface was exposed 20 (circles) or 80 (triangle) times to the vanadium precursor before the water pulse. The physisorbed species remained rather constant

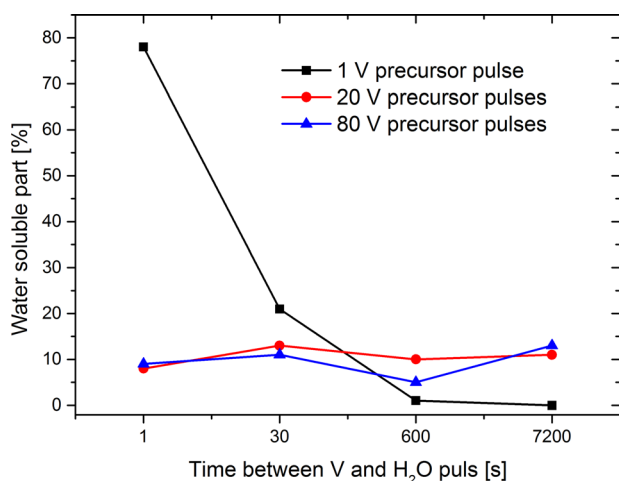


Fig. 7. (Color online) Amount of water soluble vanadium species (CVD, physisorbed) deposited on MWCNT correlated to purging time between vanadium precursor and coreactant pulse determined via ICP-OES. The effect of repeating vanadium pulses before the coreactant pulse is also visualized (rectangle: 1 exposure; circle: 20 exposures; and triangle: 80 exposures).

between 7% and 12%. This value can also be influenced by dissolving amorphous carbon. If the MWCNT surface is exposed only once to the vanadium precursor (rectangle) before the water pulse, a significant influence on the ratio between physisorbed (CVD) and chemisorbed (ALD) vanadium can be detected. The physisorbed contribution varies between 2% and 80%. With increasing purging times between the precursor and water pulse, the physisorbed contribution decreases. The high amount of physisorbed vanadium species at short purging times is a hint that a gas phase reaction between the vanadium precursor and the coreactant (water) had occurred. During this process, no covalent bond between the MWCNT and vanadium oxide was formed; accordingly, no ALD process happened although a deposition took place.

The existence of single site vanadium oxides on the MWCNT surface was proven via Raman spectroscopy and high resolution scanning transmission electron microscopy (HRSTEM) imaging. In Raman spectroscopy, single site vanadium oxide does not exhibit a characteristic lattice vibration.^{20,21} The Raman spectra of various loadings of vanadium oxide are shown in Fig. 8. To visualize the characteristic V_2O_5 lattice vibration, a MWCNT sample with a low amount of vanadium oxide was heated up to 350 °C in oxygen to destroy the single-site structure of the vanadium oxide (Fig. 8, first from the top). Raman shifts in the 100–200 cm^{-1} range are assigned to V–V interactions and to V–O–V vibrations in the range between 300 and 700 cm^{-1} .^{20,21} MWCNT samples with small vanadium oxide loadings do not exhibit any signal in the range of the V–O–V vibrations. Despite, signals corresponding to V–V interactions in the range of 100–200 cm^{-1} are slightly visible. These signals result from neighboring vanadium species due to areas of high density of functional groups on the MWCNT where covalent bonds could be formed. Additionally, the spectra exhibit a shoulder at 1025 cm^{-1} which can be assigned to lattice V=O stretch vibrations.²⁰ This supports the suggestion that interactions occur between neighboring vanadium oxides. With increasing vanadium oxide concentrations, a broad signal appears among 800–1000 cm^{-1}

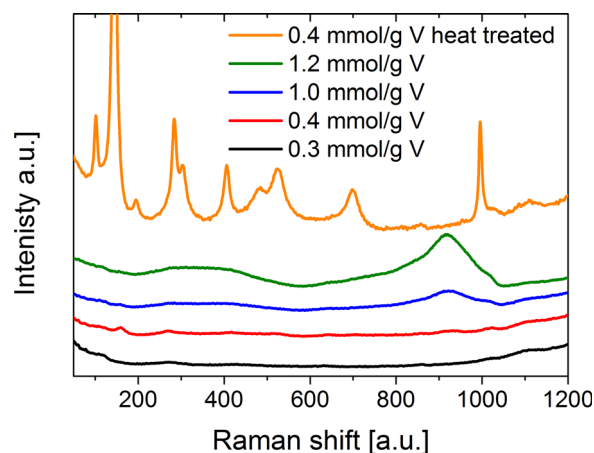


Fig. 8. (Color online) Raman spectra of vanadium oxide MWCNT composite materials with different vanadium loadings. Heat treated composite material (first from the top) to visualize lattice vibration of V_2O_5 vibration on MWCNT.

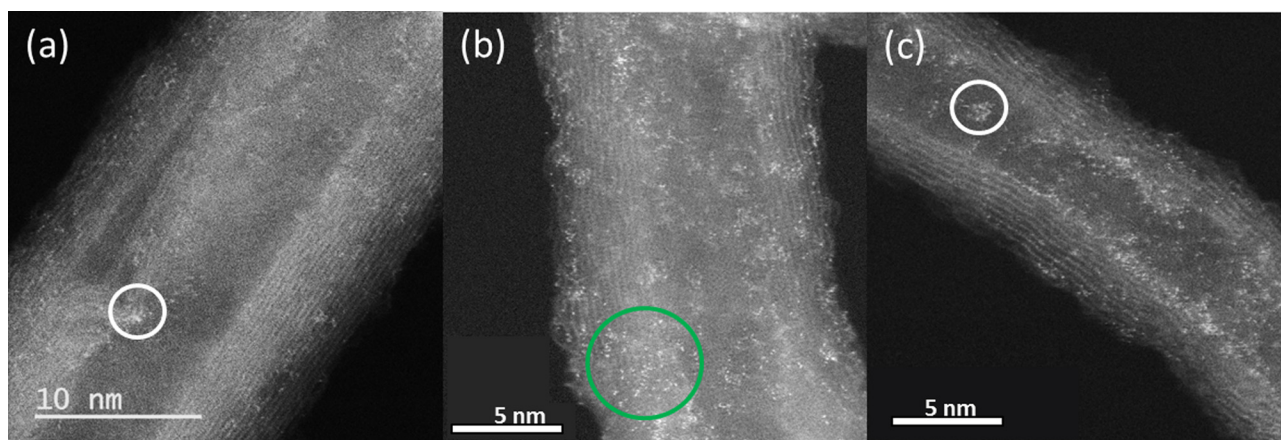


Fig. 9. (Color online) HRSTEM images of different vanadium oxide loadings [(a) 0.3 mmol/g; (b) 1.0 mmol/g; and (c) 1.4 mmol/g] on nitrosulfuric acid pretreated MWCNT. Areas of high density of reactive functional groups and therefore high amounts of vanadium oxide species [circles in (a),(c)] and areas of highly distributed active functional groups that lead to atomically dispersed vanadium oxide species [circle in (b)].

which can be assigned to several different vibrations arising from V-OH stretches or V-O-R vibrations whereas the R represents remaining organic residuals of the vanadium precursor. Incomplete exchange of the isopropyl oxide accordingly to the NMR experiments shown in Fig. 4 with water as coreactant during the ALD process might happen. Consequently, exact identification of the deposited vanadium species is not possible and the ligand exchange reaction during the second ALD cycle cannot be optimized via the use of Raman spectroscopy. An uncomplete exchange of organic ligands of the vanadium precursor will have a negative impact on the growth rate when applying more ALD cycles as well as the material properties will be influenced due to organic residuals in the vanadium oxide film. Therefore, following studies with increasing numbers of ALD cycle with the focus on the exchange reaction of organic residuals have to be investigated in detail.

HRSTEM images confirm the results of the Raman measurements. Figure 9 illustrates the single site character [circle in Fig. 9(b)] of the loaded vanadium oxide MWCNT samples [(a) 0.3 mmol/g; (b) 1.0 mmol/g; (c) 1.4 mmol/g). It is shown that the vanadium species are distributed on the whole MWCNT surface in dependence of the distributed reactive functional groups. Areas with higher amounts of defects (functional groups) exhibit agglomeration of vanadium oxide species [circles in Figs. 9(a) and 9(c)], whereas areas with more graphitic structure shows predominately single site vanadium species. The visualization of distributed ALD active functional groups is therefore also possible as shown by the TEM images.

IV. SUMMARY AND CONCLUSIONS

In this work, vanadium oxide was deposited on pretreated MWCNT. Due to parameter changes, it was evident that the pretreatment of MWCNTs has a large influence on the deposition process. The variation of deposition parameters shows that functional groups are not mandatory for deposition to occur. However, a chemical bond between the MWCNT and vanadium precursors could only be formed when functional groups were present. The activity of different functional groups concerning the ALD process was investigated via

various methods. TG-MS analysis revealed a consumption of carboxylic, anhydride, and phenol groups upon exposure to the vanadium precursor. These results are confirmed by electronic structure theory calculations and grafting experiments analyzed via ^{51}V NMR. The nature of the deposited vanadium species varies from completely $[\text{O}=\text{V}(\text{OH})_2]$ over partial $[\text{O}=\text{V}(\text{OH})(\text{isopropyl})]$ to not $[\text{O}=\text{V}(\text{isopropyl})_2]$ hydrolyzed.

We have described the influence of several ALD parameters on the consumption of the carboxylic group and found the optimal deposition conditions for ALD of vanadium oxide: 0.35 s vanadium precursor pulse, 150°C deposition temperature, and 10 min of purging between vanadium precursor and water pulses. Through this procedure, we have deposited immobilized atomically dispersed vanadium oxide species onto MWCNT surfaces.

The immobilization was investigated via ICP-OES, revealing the water- and acid-soluble vanadium oxide part on the MWCNT, representing the physisorbed species according to CVD and covalently bonds species according to ALD. It was shown that traditional short precursor exposures and short purging times between vanadium precursor and oxygen source results primarily in physisorbed metal species. With an increase in precursor pulses and purging times, this effect could be minimized.

Raman spectroscopy as well as HRSTEM images confirmed the existence of atomically dispersed vanadium oxide species on the MWCNT surface. With increasing exposure time, the homogeneity of the deposited vanadium oxide increases. Defect structures, where higher densities of active functional groups are present in the graphitic lattice, result in higher vanadium loadings. The described approach to characterize an ALD process can be extended for other metal precursors and support materials, where traditional characterization methods are not applicable. Especially, the characterization and optimization of ALD approaches on powder based material can be improved with this approach. With the present applied methods like quartz crystal microbalance, one can answer questions concerning the presence of deposited species and their deposition rate that adsorb without bond formation during an ALD process. A differentiation

between ALD and CVD processes and therefore physisorbed or covalently bonded species is impossible. Selectively deposited species on support materials opens a broad field for fundamental investigation of active sites and their performance as well as stability in catalytic processes.

ACKNOWLEDGMENTS

The authors would like to thank Thomas Weyhermüller for NMR measurements. Also thanks to Birgit Deckers for the support in graphical design. A.A.A., K.H.B. and I.S. would like to acknowledge the MPG MAXNET Energy initiative for financial support.

- ¹S. Banerjee, T. Hemraj-Benny, and S. S. Wong, *Adv. Mater.* **17**, 17 (2005).
- ²A. Hirsch, *Angew. Chem. Int. Ed.* **41**, 1853 (2002).
- ³D. B. Farmer and R. G. Gordon, *Nano Lett.* **6**, 699 (2006).
- ⁴J. Li, S. Tang, L. Lu, and H. C. Zeng, *J. Am. Chem. Soc.* **129**, 9401 (2007).
- ⁵D. B. Farmer and R. G. Gordon, *Electrochem. Solid-State Lett.* **8**, G89 (2005).
- ⁶C. Wang, M. Waje, X. Wang, J. M. Tang, R. O. Haddon, and Y. Yan, *Nano Lett.* **4**, 345 (2004).
- ⁷T. Helbling, C. Hierold, C. Roman, L. Durrer, M. Mattmann, and V. M. Bright, *Nanotechnology* **20**, 434010 (2009).

- ⁸X. Liang, D. M. King, P. Li, and A. W. Weimar, *J. Am. Ceram. Soc.* **92**, 649 (2009).
- ⁹M. Willinger, G. Neri, A. Bonavita, G. Micali, E. Rauwel, T. Hertrich, and N. Pinna, *Phys. Chem. Chem. Phys.* **11**, 3615 (2009).
- ¹⁰P. Dungen, M. Prenzel, C. Van Stappen, N. Pfänder, S. Heumann, and R. Schlögl, *Mater. Sci. Appl.* **8**, 628 (2017).
- ¹¹K. Balasubramanian and M. Burghard, *Chem. Unserer Zeit* **39**, 16 (2005).
- ¹²X. Chen, E. Pomerantseva, P. Banerjee, K. Gregorczyk, R. Ghodssi, and G. Rubloff, *Chem. Mater.* **24**, 1255 (2012).
- ¹³See supplementary material at <https://doi.org/10.1116/1.5006783> for ALD procedure, Grafting 1H/13C NMR, Details DFT calculation, TG-MS measurements / consumption functional groups / interaction vanadium-carbon during thermal analysis.
- ¹⁴J. L. Figueiredo, M. F. R. Pereira, M. M. A. Freitas, and J. J. M. Orfao, *Carbon* **37**, 1379 (1999).
- ¹⁵Q.-L. Zhuang, T. Kyotani, and A. Tomita, *Energy Fuels* **8**, 714 (1994).
- ¹⁶K. F. Ortega, R. Arrigo, B. Frank, R. Schlögl, and A. Trunschke, *Chem. Mater.* **28**, 6826 (2016).
- ¹⁷B. Marchon, W. T. Tysoe, J. Carrazza, H. Heinemann, and G. A. Somorjai, *J. Phys. Chem.* **92**, 5744 (1988).
- ¹⁸P. J. Hall and J. M. Calo, *Energy Fuels* **3**, 370 (1989).
- ¹⁹T. Liseč, T. Reimer, M. Knez, S. Chemnitz, A. V. Schulz-Walsemann, and A. Kulkarni, *J. Microelectromech. Syst.* **26**, 1093 (2017).
- ²⁰S. Boukhalfa, K. Evanoff, and G. Yushin, *Energy Environ. Sci.* **5**, 6872 (2012).
- ²¹R. Baddour-Hadjean, M. B. Smirnov, K. S. Smirnov, V. Yu Kazimirov, J. M. Gallardo-Amres, U. Amador, M. E. Arroyo-de Dompablo, and J. P. Pereira-Ramos, *Inorg. Chem.* **51**, 3194 (2012).